International Journal of Science and Research (IJSR)
ISSN: 2319-7064
SJIF (2022): 7.942

Synthesis and Post Modification of SBA-16 Mesoporous Molecular Sieves with Different Si/Al and Si/Ti Ratios

S. B. Shete

Department of Physics, S.G.B. College, Purna (Jn) – 431 511
Email: *s.bshete[at]rediffmail.com*

Abstract: ***Spherical particles of mesoporous silica SBA-16 with cubic Im3m structure were synthesized at low pH using Pluronic F127 as template and Rice husk (RHA) as silica source. The diameter of the spherical particles can be controlled in the range of 0.5-8 µm by varying Spherical particles of mesoporous silica SBA-16 with cubic Im3m structure were synthesized at low pH using Pluronic F127 as template and RHA as silica source. The diameter of the spherical particles can be controlled in the range of 0.5-8 µm by varying synthesis temperature t 45 °C. A sharp transition from large particle is observed. It is suggested that this morphology transition is due to a change in hydrolysis and condensation rate of the silica source and as a result the assembly of F127 micelles will differ. The SBA-16 samples were characterized using powder X-ray diffraction (XRD), scanning electron microscopy (SEM),transmission electron microscopy (TEM) and Nitrogen adsorption techniques.***

Keywords: SBA-16; Spherical particles; Synthesis temperature; Morphology; F127

1. Introduction

Spherical particles of mesoporous silica SBA-16 with cubic Im3m structure were synthesized at low pH using Pluronic F127 as template and RHA as silica source. The diameter of the spherical particles can be controlled in the range of 0.5–8 µm by varying. The synthesis of mesoporous materials by a liquid-crystal template mechanism was reported (Beck J.S., *et al* 1992, Kresge C.T., *et al* 1992). The properties of these materials make them attractive for adsorption, catalysis, separation, chemical sensing, optical coating, drug delivery and electronic applications. For practical purposes, the overall morphology of a mesoporous material is a necessary requirement in combination with their internal structure. SBA-16 is a mesoporous material with 3D cubic pore arrangement corresponding to Im3m space group (Boissiere C., *et al* 2001). In this body-centred-cubic structure each mesoporous is connected with its eight nearest neighbours to form a multidirectional system of mesoporous network (Sakamoto Y, *et al* ,2000), Due to its large cage, high surface area and high thermal stability. (Hudson SP., *et al*2008), this material appears to be one of the best candidates for catalytic support and packing materials for separation. Using F127 as a surfactant is the common way of synthesizing SBA-16(Zhao D., *et al* 1998, Van der Voort P. *et al* 2002). However, there are also reports on alternative surfactants such as F108 (Kipkemboi P., *et al* 2001), a blend of P123 and F127.

Micro porous zeolite are widely used as solid acid catalysts, (Shaodian Shen, *et al* 2007) but their applications are intrinsically limited by drawback of zeolite is that the small size of the channels (less than 0.8 nm) and cavities (<1.5 nm) imposes diffusion limitations on reactions that can cause high back pressure on flow systems. The dimensions of the zeolite micro pores (< 2 nm), mesoporous (2-50nm) and macro pores (> 50 nm) permit faster migration of guest molecules in the host frameworks. Since fast mass transfer of the reactants and products to and from the active sites is required for catalysts (Kresge C.T., *et al* 1992), the concept of infusing mesoporous into zeolite particles has attracted much attention. Recent progress involving this issued to ordered mesoporous materials such as MCM-41, SBA-16 and SBA 15. These mesoporous materials have pore diameters of 3.0 nm– 8.0nm and exhibit catalytic properties for the catalytic conversion of bulky reactants, but unfortunately, when compared with micro porous zeolite (Kecht J., *et al*, 2008), the catalytic activity and hydrothermal stability are relatively low, which can be attributed to the amorphous nature of the mesoporous walls. To overcome this problem, some recent research efforts have been concentrated on introducing mesoporous or macro pores linked to the zeolite micro pores. These materials called Hierarchical zeolite materials with combinations of micro/meso/macro pores would further extend the application of zeolite as solid acid (Van der Voort P., *et al* 2002).

2. Material and Methods

SBA composite with different concentrations have been prepared under acidic conditions in the presence of triblock copolymer F127 by using RHA as silica source 1.6gm of F127was dissolved in 120gm of H2O,5gm of conc. HCL and 7.5gm of butanol under magnetic stirring 1h to obtain homogeneous solution at 45^0C to this solution 4.5gm of RHA was added. The mixture was stirred for another 24 hours. Ultrasonic treatment is given at power 70 for 30 min Then the solution is taken Teflon coated autoclave and hydrothermal treatment is given to 80^0C for 24 hrs. The synthesized mesoporous composite was filtered and dried in air. The sample is calcined at 1.5°C/ min .at 550^0C for 6h (Carniato Fabio *et al* 2012).

3. Result and Discussion

XRD-studies:

As-synthesized forms of RHA-SBA-16 (60, 70, 80 and 90) exhibit a typical pattern with a very strong (110) reflection at low angle $1.14^0$and other weaker reflections as shown in Fig.1 A-(70, 80). According to Beck *et.al*these reflection lines can be indexed based on a hexagonal unit cell parameter (a_0= √2d110). In the XRD pattern of the calcined RHA-SBA-16(60^0C), only the (110) reflection is observed prominently. The presence of only (110) reflection in the calcined sample suggests that this material does not possess the well- defined hexagonal arrays after calcinations. In both the as-synthesized and calcined samples, the mainly strong peak with (110) reflection is swung to higher d_{110}spacing values with increase in temperature of hydrothermal synthesis from 60^0C to 90^0C and afterwards it lowers (Fig.1A) and (Fig.1 B).

The sample RHA-SBA-16(80) in its as-synthesized form shows a different XRD pattern as in Fig. 1-A. The higher angle peaks due to (110) and other reflections are likely to fuse together forming one broad peak. This is due to the instability of the sample at the higher temperature, required for the removal of surfactant molecules present between the silicate sheets.

% Crystallinity and Activation Energy:

The percent crystallinity of the samples drawn at different synthesis temperatures in the crystallization kinetic was obtained by the following relation.

$$\% \text{ Crytallinity} = \frac{\text{Sum of the peak heights of unknown material} \times 100}{\text{Sum of peak heights of standard material}}$$

Table 1 summarizes the values of inter planar spacing (d values) derived from X-ray diffraction pattern for RHA-SBA-16 (100 % crystalline) and was used as a parent sample for further study. The kinetic curve describing the increase in the crystallinity of the crystals with the synthesis temperature (before and after calcination) is nearly "S" shaped that depends on rate of conversion. This type of sigmoidal nature of crystallization curve indicates two distinct stages, namely an induction period and a crystal growth period. It is seen from the Fig. 1 (C)that up to 60^0C the rate of conversion of amorphous to crystallization of RHA-SBA-16 phase was initially slow and then it increased sharply between 70^0C to 80^0C followed by subsequent slow down. By the application of Arrhenius equation to the kinetics of crystallization of RHA-SBA-16, apparent activation energy of conversion of aluminosilicate gel to 100% crystalline phase was found to be 106.12kJmole^{-1} in the present crystallization system.

BET surface area and pore volume of RHA-SBA-16

The samples synthesized at different temperatures have also been characterized by N2-adsorption-desorption study. The isotherms obtained from N2-adsorption-desorption and corresponding BJH pore size distribution is shown in Fig. 2 (A, B). According to IUPAC classification, these isotherms of RHA-SBA-16 are of type IV, which is the characteristic of mesoporous material. The isotherms exhibit three stages. The first stage is a linear part almost going through the origin, which is due to monolayer adsorption of nitrogen on the walls of the mesoporous (p/p0 < 0.2). The second stage is characterized by a steep increase in adsorption (within the relative pressure p/p0 range of 0.2-0.4) due to capillary condensation of N2 in the pore channels. This part shows hysteresis. For Samples RHA-SBA-16 (60) and RHA-SBA-16 (80), a linear increase in adsorption at low pressures is observed followed by a steep increase in nitrogen uptake [at a relative pressure of p/p_0= 0.31-0.41 and 0.25-0.35 for RHA-SBA-16(60) and RHA-SBA-16(80), respectively due to capillary condensation inside the mesoporous Fig. 2 (A) for RHA-SBA-16(60, 70, 80). The broad hysteresis loop in the isotherm for RHA-SBA-16(60) reflects disorder in the shape and size of the mesoporous. This step of the isotherm is sharper for RHA-SBA-16(80) indicating a narrow pore size distribution. Thus, as the crystallization temperature increases from 60^0C to 80^0C, the step of the isotherm becomes sharper indicating narrower pore size distribution Fig. 2 (B) for RHA-SBA-16 (60, 70, and 80). The N2-adsorption-desorption isotherms and the pore size distribution of the Sample RHA-SBA-16 (90) are found that the hysteresis loop is a wide range of relative pressures, p/p_0 (0.28-1.00). The shape of the hysteresis loop confirms the formation of a lamellar phase. The pore size distribution becomes broader. Thus, the XRD results are confirmed by N2-adsorption-desorption data, which are similar to those, reported for SBA-16. In pore size distribution curve, narrow and sharp peak is observed in the diameter range 20-25 Å showing uniform pore size. The isotherms of the RHA-SBA-16 samples show small hysteresis loop in the lower pressure regions. We noted that the surface areas of calcined RHA-SBA-16samples are comparatively more than as synthesized RHA-SBA-16 and it is increasing with the increase in crystallization temperature. The more surface area (788.6m^2/g) is an indication of well narrow dispersion of pores.

Table 1 presents a summary of all the parameters obtained by nitrogen sorption and powder X-ray diffraction pattern. The unit cell parameter (a_0) has been calculated by the formula a_0 = √2 d110. The wall thickness has been calculated by subtracting the pore diameter obtained from N2-sorption from the unit cell parameter (a_0). It is observed from the tabulated data that spacing value of most intense peak at d_{110} is slightly increase and the pore diameter is decreased with increase in temperature of hydrothermal synthesis from 60^0C to 80^0C. It is due to increase in the wall thickness of the pores of RHA-SBA-16. The surface area is increased with the increase in synthesis temperature from 60^0C to 90^0C due to the progressive formation of ordered mesophase silica. However, the surface area decreases with further increase in synthesis temperature due to silica pore shrinkage. This suggests that increasing the synthesis temperature can accelerate the silicate condensation on the silica wall, which subsequently thickens the silica framework.

Thus, the above results indicate that in hydrothermal synthesis of RHA-SBA-16 molecular sieves, temperature plays a significant role. An increase of the crystallization temperature from 60^0C to 80^0C increases the long-range

order in the structure as well as the wall thickness of the RHA-SBA-16 molecular sieves. However, with further increase in the temperature to 90^0C, the hexagonal phase changes to a lamellar one under the synthesis conditions.

SEM and TEM-Analysis:

SEM images of RHA-SBA-16(60, 80) are depicted in Fig.4 represents that the ensuing particles are roughly spherical in shape with no agglomerations. Small spherical particles are of RHA-SBA-16(80) with diameters of 7.6 to 18.4A^0.

It is observed that the average diameter of the particles is slightly increased as the synthesis temperature is elevated from 60^0C to 90^0C after calcinations. However, when the synthesis temperature was around 80^0C, the prepared sample has signified a high-quality structural morphology.

Table 1: Effect of crystallization temperature on Structural and textural properties of RHA-SBA-16

As synthesized Samples	d_{110}	Unit cell parameter	S.A. (m^2/g)	Average pore diameter(Å)	Pore volume (ml/g)	Average Wall thickness (Å)	% Crystal- lanity
RHA-SBA-16(60)	20.13	28.99	217.22	--	-	--	10
RHA-SBA-16(70)	21.51	30.97	326.42	--	-	--	22
RHA-SBA-16(80)	23.44	33.75	701.35	25.32	0.416	8.43	71
RHA-SBA-16(90)	23.12	33.29	606.70	24.91	0.488	8.38	67
For Calcined Samples							
RHA-SBA-16(60)	23.43	33.74	664.34	25.63	0.492	8.11	41
RHA-SBA-16(70)	25.55	36.79	711.65	27.33	0.523	9.46	60
RHA-SBA-16(80)	26.93	38.78	779.70	29.16	0.568	9.62	100
RHA-SBA-16(90)	23.68	34.10	689.21	25.21	0.501	8.89	87

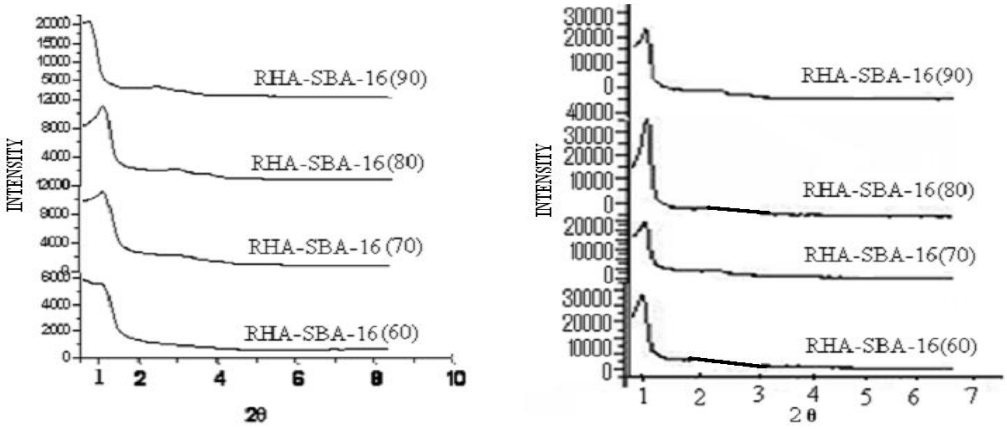

Figure 1: XRD patterns of (A) as-synthesized and (B) calcined samples of RHA-SBA-16(60^0C to 90^0C) for synthesis temperatures 60^0-90^0C

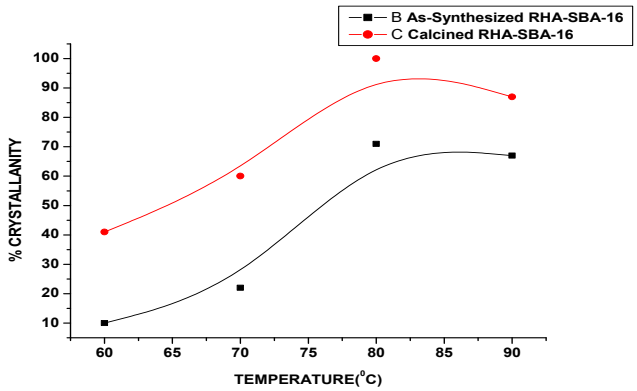

Figure 2: (C) Effect of synthesis temperature on crystallization

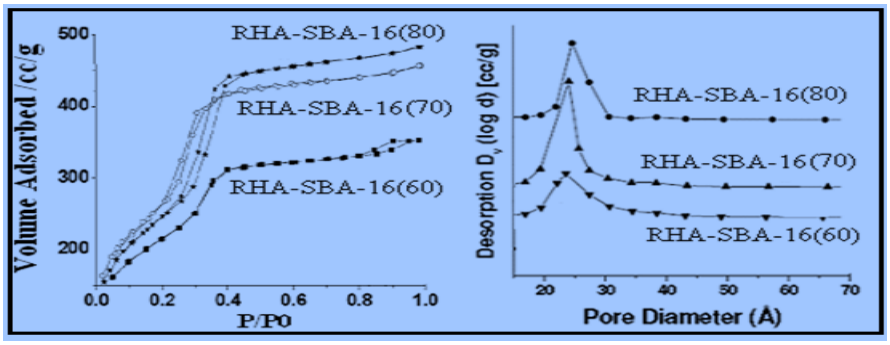

(A) (B)

Figure 3: (A) N_2 adsorption-desorption isotherms and (B) pore size distribution of RHA-SBA-16 (60, 70, 80) synthesized at 60^0-80^0C

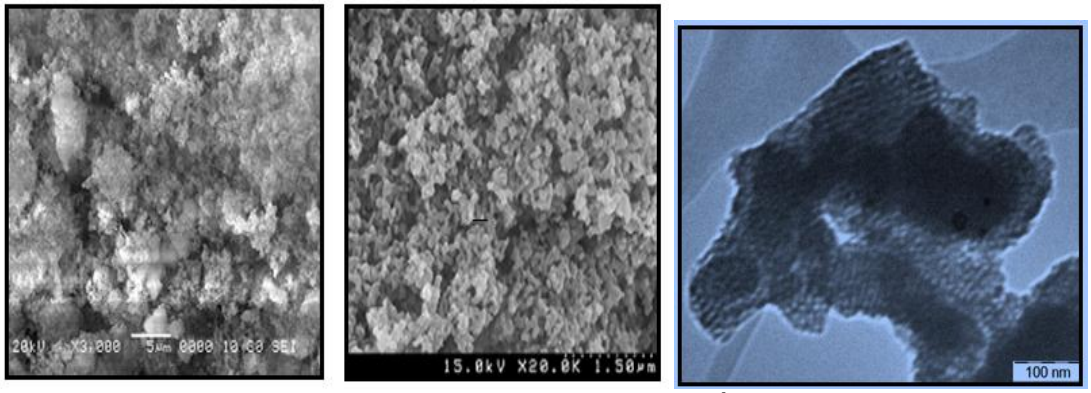

Figure 4: SEM images of RHA-SBA-16(60, 80) synthesized at 60 and 80^0C Fig. 5: TEM images of RHA-SBA-16(80) synthesize

Post Synthesis Modification of RHA-SBA-16 by Al^{+3} metal ions:

In both post synthesis modification that is the preparation of Al-RHA-SBA-16 and Ti-RHA-SBA-16 the direct synthesis method is used. Aluminium isopropoxide as Al pre cursor was employed for Al incorporation into the silica frame work. The pH of the gel was kept low so to effective incorporation of Al. The aqueous solution of Al^{+3} was added drop by drop in hydrothermal synthesis gel prepared as described in the earlier section different concentration of Alumina (in gel Si/Al = 4,7, 9). The samples obtained after the filtrations are dried at room temperatures and calcined at 550^0C for 8 h. This samples are designated as Al-RHA-SBA-16 (in gel Si/Al = 4,7,9) and this samples are characterized X-RD, EDAX, SEM, FTIR. The obtained Si/Al ratio tabulated in table 2

Post Synthesis Modification of RHA-SBA-16 by Ti^{+4} metal ions:

Titanium isopropoxide as Ti pre cursor was employed for Ti incorporation into the silica frame work. The pH of the gel was kept low so to effective incorporation of Ti. The aqueous solution of Ti^{+4} was added drop by drop in hydrothermal synthesis gel prepared as described in the earlier section different concentration of titanium (in gel Si/Ti = 2, 4, 6). The samples obtained after the filtrations are dried at room temperatures and calcined at 550^0C for 8 h. This samples are designated as Ti-RHA-SBA-16 (in gel Si/Ti = 2, 4, 6) and this samples are characterized X-RD, EDAX, SEM, FTIR. The obtained Si/Ti ratio tabulated in table 2.

4. Results and Discussion

1) Energy Dispersive Analysis of X-ray (EDAX):

Table 2: Elemental Composition of the Samples Analyzed by EDAX

Sample name	Si	Al	Si/Al ratio	Ti Metal ion wt%
Al-RHA-SBA-16 (in gel:Si/Al=4)	56.81	14.68	Si/Al=3.87≈ 4	_
Al-RHA-SBA-16 (in gel Si/Al=7)	64.62	9.42	Si/Al=6.86 ≈7	_
Al-RHA-SBA-16 (in gel Si/Al=9)	69.30	7.83	Si/Al=8.85 ≈ 9	_
Ti-RHA-SBA-16 (in gel Si/Al=2)	68.47	1.74	_	Ti =1.91 ≈2
Ti-RHA-SBA-16(in gel Si/Al=4)	63.71	1.78	_	Ti =3.83 ≈ 4
Ti-RHA-SBA-16 (in gel Si/Al=6))	64.11	1.81	_	Ti =5.76 ≈6

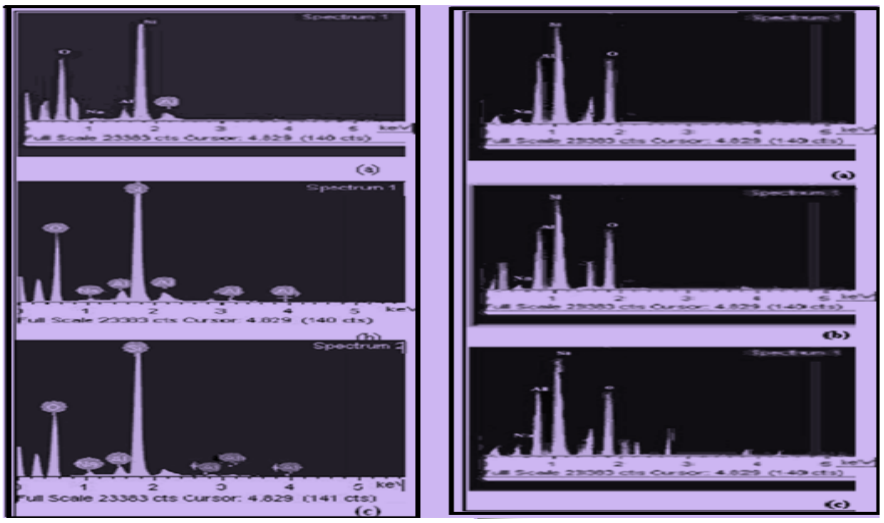

(A) (B)

Figure 6: (A) EDAX IMAGES OF (a) Al-RHA-SBA-16 (Si/Al=4), (b) Al-RHA-SBA-16 (Si/Al=7) and (c) Al-RHA-SBA-16 (Si/Al=9).
(B) EDAX IMAGES OF (a) Ti-RHA-SBA-16 (gel Si/Ti =2), (b) Ti-RHA-SBA-16 (gel Si/Ti =4) and (c) Ti-RHA-SBA-16 (gel Si/Ti =6).

X-ray diffraction (RHA-SBA-16, Al-RHA-SBA-16, Ti-RHA-SBA-16)

This section gives detailed information on characterization data of the RHA-SBA-16, Al-RHA-SBA-16 and Ti-RHA-SBA-16 samples with different Si/Al ratios and with different mole ratio of Ti- exchanged respectively.

The XRD patterns of the calcined parent RHA-SBA-16, Al-RHA-SBA-16 and Ti-RHA-SBA-16 samples with different Si/Al ratios in gel (4, 7 and 9) and with different Si/Ti ratios in gel (2, 4, and 6) respectively are presented in Fig. 7 (A, B, C) respectively.

The spectra showed XRD patterns identical to that reported for standard SBA-16 materials. Beck*et al*. indexed these peaks for a hexagonal unit cell, the parameter of which was calculated from the equation $a_0 = \sqrt{2}d_{110}$.Oncalcination of samples, the peak is shifted to lower d_{110} spacing value probably due to condensation of internal Si-OH groups giving rise to a contraction of the unit cell. The unit cell parameter and d-spacing of the Al-RHA-SBA-16, Ti-RHA-SBA-16 samples and RHA-SBA-16 are given in Table 2.

The slight increase in d-spacing and unit cell parameters of both Al-RHA-SBA-16 and Ti-RHA-SBA-16 compared to RHA-SBA-16 suggests the presence of Aluminum and Titanium in the framework respectively. The increase in unit cell parameter on Al or Ti incorporation is probably due to the replacement of shorter Si-O bonds by longer Al-O and Ti-O bonds in the structure respectively. It is also observed that along with an increase in the unit cell parameter, the (110) diffraction peak becomes broader and less intense with increasing Aluminum or Titanium content, probably because of the change of the Al-O-Al and Ti-O-Ti bond angle, causing a distortion in the long range ordering of the hexagonal mesoporous structure.

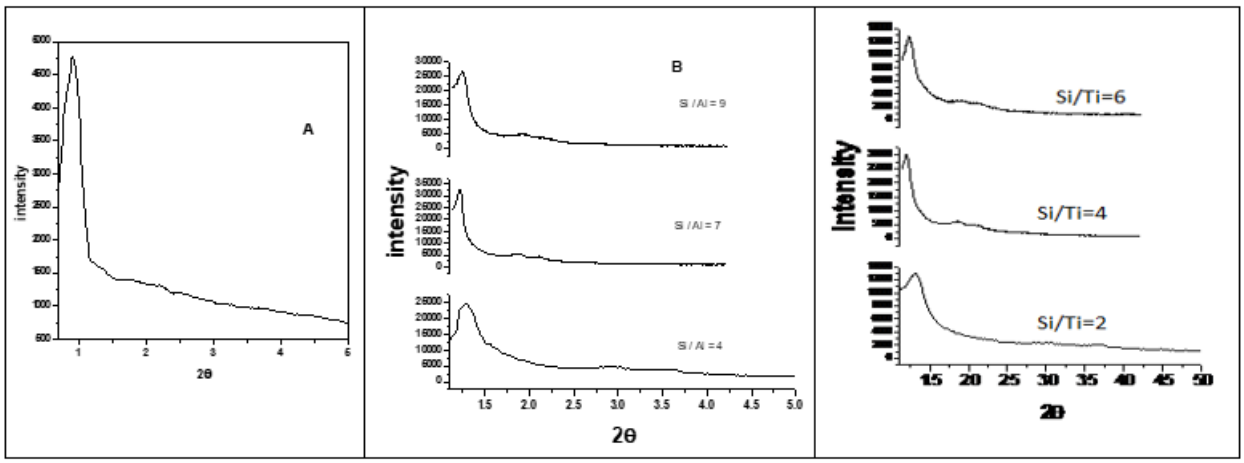

Figure 7: (A) XRD patterns of calcined parent RHA-SBA-16 sample. B) Al-RHA-SBA-16 (i.e. Si/Al=4, 7, 9) C) Ti-RHA-SBA-16 (Si/Ti=2,4,6)

Fig. 7 (B, C) illustrate that in all the modified forms of RHA-SBA-16 sample, there are marginal changes in the crystallinity but almost no changes in the phase purity and structural morphology are being observed after modification with different amounts of Al^{+3} and Ti^{+4} percentage. This indicates the structural stability of the parent sample and

presence of metal ions in the intra-crystalline voids of the RHA-SBA-16. The percent crystallinity of the samples is drawn with the amount of metal ion percent in them. From the Table 2.12 as the metal ions percent increases in modification, an increase in the crystallinity of the samples was observed up to Si/Al=4 and Si/ Ti=6. But when Si/Al > 4 and Si/Ti > 6 i.e. when the metal ion concentration increases then the sample declines from good crystallinity to amorphous nature. This is because of the fact that, Al itself is having an amorphous nature and Ti being strong earth metal it produces other amalgamations in the structure influencing the crystallinity, hence the modification was stopped after Si/Al=4 and more than Si/Ti=6 incorporation to retain the crystallinity of the sample. The crystallinity of the sample was 100% for RHA-SBA-16. If the 'Al' metal ion concentration in RHA-SBA-16 was Si/Al = 4 crystallinity was 98.5% and then gradually decreased for Si/Al=7, 9 as 91.3% and 86.5% respectively. However, if the 'Ti' metal ion concentration in RHA-SBA-16 was 6 it was 96.5% and then gradually decreased for 4 and 2 as 84.3% and 80.4% respectively.

Fig. 8 depicts the co-relation between % crystallinity and concentration of Al and Ti metal ions.

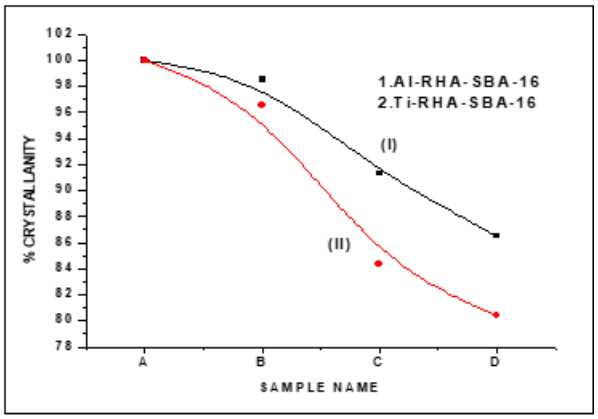

Figure 8: Effect of the metal concentration on Percent Crystallinity of RHA-SBA-16

Table 3: Physicochemical properties of Al-RHA-SBA-16 and Ti-RHA-SBA-16 samples

Sample	d_{110}	Surface Area (m^2/g)	Pore Volume(ml/g)	Pore diameter(A^0)	% Crystallanity	Acidity (mmole/g)
RHA-SBA-16	33.16	954.22	0.65	27.3	100	0.014
Al-RHA-SBA-16 (Si/Al=4)	33.32	852.00	0.76	28.6	98.5	0.192
Al-RHA-SBA-16 (Si/Al=7)	34.62	826.46	0.71	31.2	91.3	0.086
Al-RHA-SBA-16 (Si/Al=9)	35.75	938.61	0.69	26.8	86.5	0.044
Ti-RHA-SBA-16 (Si/Ti =2)	45.56	789.36	0.62	30.9	80.4	0.017
Ti-RHA-SBA-16 (Si/Ti =4)	45.85	809.58	0.68	30.4	84.3	0.019
Ti-RHA-SBA-16 (Si/Ti =6)	45.58	926.25	0.72	29.8	96.5	0.024

5. Conclusion

The correlation of the work reported by (Carniato Fabio *et al* 2012).is using commercially available chemicals but our research is by using low cost waste material. We got the same result as reported.

All the characterization techniques performed in this study reveals that well ordered mesoporous material of uniform hexagonal array can be synthesized very conveniently and in a very short span of time from an agro waste rice husk ash instead of commercial expensive silica sources. The parametric variation such as change of synthesis temperature helps to optimize the synthesis conditions. The well ordered mesoporous material RHA-SBA-16 can be synthesized at 80^0C for 4.5h keeping pH of gel 6.9 and calcined at 550^0C.The apparent activation energy of conversion of synthesis gel to 100 % crystalline RHA-SBA-16 phase was 184.62kJ/mole calculated by Arrhenius equation.

Referances

[1] Beck J.S., Vartuli J.C., Roth W.J., Leonowicz M.E., Kresge C.T., Schmitt K.D., W Chu C.T., D.H. Olson, E.W. Sheppard, S.B. McCullen, J.B. Higgins, J.L. Schlenker, (1992). A New Family of Mesoporous Molecular Sieves Prepared with Liquid Crystal TemplatesJ. Am. Chem. Soc.; 114: 10834–43.

[2] Boissiere C., Kummel M., Persin M., Larbot A. and Prouzet E., Adv. Funct. Mater. (2001). Porosity and Mechanical Properties of MesoporousThinFilms Assessed by Environmental Ellipsometric Porosimetry. 129

[3] Carniato Fabio, Paul Geo, Stefano Chiara BisioCaldarelli and Marchese Leonardo (2012), On the organic/inorganic interface between mesoporous SBA-16 silica and its structuraldirecting polymer: a combined FT-IR and solid state NMR study 1153–1160

[4] Hudson SP, Padera RF, Langer R, Kohane DS. (2008) The biocompatibility of mesoporous silicates. Biomaterials. 29:4045–55.

[5] Kecht J, Schlossbauer A, Bein T. (2008) Selective functionalization of the outer and inner surfaces in mesoporous silica nanoparticles. Chem Mater; 20:7207–14.

[6] Kipkemboi P., Fogden A, Alfredsson V. Flodström K. Langmuir 17 (2001) Triblock Copolymers as Templates in Mesoporous Silica Formation: Structural Dependence on PolymerChain Length and Synthesis Temperature5398.

[7] Kresge C.T., Leonowicz M.E., Roth W.J., Vartuli J.C., Beck J.S., (1992) Nature 359 Orderedmesoporous molecular sieves synthesized by a liquid-crystal template mechanism 710.

[8] Sakamoto Y., Kaneda M., Terasaki O., Zhao D.Y., Kim J.M., Stucky G., Shin H.J., Ryoo R., Nature 408 (2000) 449.

[9] ShaodianShen, Deng Yan, Zhu Guibo, Dongsen Mao; Wang Yuhong, Guishen Wu, Jun Li.XiaoZhenLiu, Guanzhong Lu, Zhao Dongyuan. (2007) J Mater Sci.A Zeolite-Like Zinc Phosphonocarboxylate Framework and Its Transformation into Two- and Three-Dimensional Structures 7057–7061

[10] Van der Voort P., Benjelloun M, Vansant E.F, (2002) Rationalization of the synthesis of SBA-16: controlling the micro- and mesoporosity. J. Phys. Chem. B 106 9027.

[11] Zhao D., Huo Q., Feng J., Chmelka B.F., Stucky G.D, (1998) J. Am. Chem. Soc. 120 Triblock-Copolymer-Directed Syntheses ofLarge-Pore Mesoporous Silica Fibers 6024.